Citation: Molecular Therapy—Nucleic Acids (2016) 5, e381; doi:10.1038/mtna.2016.89
Official journal of the American Society of Gene & Cell Therapy
www.nature.com/mtna

Antisense Oligonucleotide-based Splice Correction for *USH2A*-associated Retinal Degeneration Caused by a Frequent Deep-intronic Mutation

Radulfus WN Slijkerman[1,2], Christel Vaché[3,4], Margo Dona[1,2], Gema García-García[4], Mireille Claustres[3,4], Lisette Hetterschijt[1,5], Theo A Peters[1,5], Bas P Hartel[1,6], Ronald JE Pennings[1,5], José M Millan[7], Elena Aller[7], Alejandro Garanto[5,8], Rob WJ Collin[5,8], Hannie Kremer[1,5,8], Anne-Françoise Roux[3,4] and Erwin Van Wijk[1,5]

Usher syndrome (USH) is the most common cause of combined deaf-blindness in man. The hearing loss can be partly compensated by providing patients with hearing aids or cochlear implants, but the loss of vision is currently untreatable. In general, mutations in the *USH2A* gene are the most frequent cause of USH explaining up to 50% of all patients worldwide. The first deep-intronic mutation in the *USH2A* gene (c.7595-2144A>G) was reported in 2012, leading to the insertion of a pseudoexon (PE40) into the mature *USH2A* transcript. When translated, this PE40-containing transcript is predicted to result in a truncated non-functional USH2A protein. In this study, we explored the potential of antisense oligonucleotides (AONs) to prevent aberrant splicing of *USH2A* pre-mRNA as a consequence of the c.7595-2144A>G mutation. Engineered 2'-O-methylphosphorothioate AONs targeting the PE40 splice acceptor site and/or exonic splice enhancer regions displayed significant splice correction potential in both patient derived fibroblasts and a minigene splice assay for *USH2A* c.7595-2144A>G, whereas a non-binding sense oligonucleotide had no effect on splicing. Altogether, AON-based splice correction could be a promising approach for the development of a future treatment for *USH2A*-associated retinitis pigmentosa caused by the deep-intronic c.7595-2144A>G mutation.

Molecular Therapy—Nucleic Acids (2016) **5**, e381; doi:10.1038/mtna.2016.89; published online 1 November 2016
Subject Category: Antisense oligonucleotides

Introduction

Usher syndrome (USH) and nonsyndromic retinitis pigmentosa (NSRP) are forms of inherited retinal dystrophies. Usher syndrome is clinically and genetically heterogeneous and by far the most common cause of inherited deaf-blindness in man, with a prevalence of approximately 1 in 6,000 individuals.[1] Based on the presence and progression of the clinical symptoms, Usher syndrome can be classified in three types: type 1 (USH1), type 2 (USH2), and type 3 (USH3). Approximately two-third of Usher syndrome patients suffer from type 2 (ref. 2), of whom up to 85% have mutations in *USH2A*.[3] USH2 patients present with congenital hearing impairment, which can be partly compensated by hearing aids or cochlear implants,[4] and retinitis pigmentosa (RP). NSRP is more prevalent than Usher syndrome, occurring in 1 per 4,000 individuals worldwide,[5] of whom up to 23% can be explained by mutations in *USH2A*.[6,7] Both USH2 and NSRP patients with mutations in *USH2A* develop night blindness in their late teens as a consequence of photoreceptor degeneration.[8] This night blindness subsequently progresses from peripheral vision loss towards legal blindness around the end of the sixth decade of life.[9] However, USH2 patients have an earlier and faster decline of visual function as compared to NSRP patients with an *USH2A* mutation.[10]

Usher syndrome and other retinal dystrophies for long have been considered as incurable disorders. However, recent preclinical studies and ongoing phase 1/2 clinical trials using gene augmentation therapy led to promising results in selected groups of Usher syndrome, Leber congenital amaurosis and retinitis pigmentosa patients carrying mutations in *MYO7A*[11–14] (ClinicalTrials.gov; NCT02065011) or *RPE65* (refs. 15–18). However, *USH2A* gene augmentation is hampered as the size of its coding sequence (15,606 bp; Genbank NM_206933) exceeds the cargo capacity of the currently available vehicles used for delivery (*e.g.*, adeno-associated or lentiviral vectors). An alternative to gene augmentation is gene correction by for instance CRISPR/Cas9-based targeted genome repair. Although promising preclinical advances have been made, gene repair is not yet fully developed for clinical applications.[19]

Mutations in *USH2A* are mostly private and so far more than 600 different mutations have been reported which are distributed all over the gene (*e.g.*, nonsense and missense mutations, deletions, duplications, large rearrangements, and variants that affect splicing (USHbases; http://www.lovd.nl/USH2A)).[20,21] However, there are a few mutations that originate from a common ancestor (*e.g.*, c.2299delG; p.Glu767fs and c.2276G>T; p.Cys759Phe) and are therefore observed more frequently.[21–23]

The last two authors are the co-senior authors.
The first two authors are the co-first authors.

[1]Department of Otorhinolaryngology, Radboudumc, Nijmegen, the Netherlands; [2]Radboud Institute for Molecular Life Sciences, Radboudumc, Nijmegen, the Netherlands; [3]Laboratoire de Génétique Moléculaire, CHU Montpellier, Montpellier, France; [4]Laboratoire de Génétique de Maladies Rares EA 7402, Université de Montpellier, Montpellier, France; [5]Donders Institute for Brain, Cognition, and Behaviour, Nijmegen, the Netherlands; [6]Radboud Institute for Health Sciences, Radboudumc, Nijmegen, the Netherlands; [7]Grupo de Investigación en Biomedicina Molecular, Celular y Genómica, and CIBERER, Madrid, Spain; [8]Department of Human Genetics, Radboudumc, Nijmegen, the Netherlands. Correspondence: Erwin Van Wijk, Department of Otorhinolaryngology, Radboudumc, Geert Grooteplein 10 6500 HB Nijmegen, the Netherlands. E-mail: Erwin.vanWyk@radboudumc.nl

Keywords: antisense oligonucleotides; genetic therapy; splice redirection; USH2A; Usher syndrome
Received 4 March 2016; accepted 7 September 2016; published online 1 November 2016. doi:10.1038/mtna.2016.89

In 2012, the first deep-intronic mutation (c.7595-2144A>G) in *USH2A* was reported for which also an ancestral event was suggested in association with the rare variant c.6049+76A>T.[24] This mutation creates a high-quality splice donor site in intron 40, resulting in the incorporation of a 152-bp pseudoexon (PE40) into the mature transcript[24] and is predicted to lead to a premature termination of translation (p.Lys2532Thrfs*56). With a 4% frequency, this deep-intronic mutation represents the second most frequent Usher syndrome type 2A-causing mutation (Usher syndrome type 2A-patient cohort from Montpellier (n = 562), unpublished data). Recently, three additional deep-intronic mutations were identified in *USH2A*,[25] emphasizing the contribution and frequency of deep-intronic mutations to the pathology of Usher syndrome. Subsequent diagnostic screening of the c.7595-2144A>G mutation in Usher syndrome patient cohorts identified multiple patients with the mutation in a homo- or compound heterozygous state.[21,24,26–30] In addition, this mutation is reported (*in trans* to p.Arg4192His) in a patient with NSRP,[26] suggesting a wide distribution of the c.7595-2144A>G mutation in both USH and NSRP patients.

In this study, we explored the potential of antisense oligonucleotides (AONs) to redirect splicing in patient-derived fibroblasts harboring a heterozygous *USH2A* c.7595-2144A>G mutation. Both in fibroblasts and in a minigene splice assay, AONs showed promising preclinical potential to correct aberrant splicing, which might be of benefit for *USH2A* c.7595-2144A>G patients in the future.

Results

The deep-intronic c.7595-2144A>G mutation in *USH2A* creates a high-quality splice donor site that leads to a partial exonification of intron 40 (152 bp; PE40) into the mature mRNA[24] (**Figure 1a**,**b**). This results in a predicted frameshift and premature termination of translation. The aim of this study is to assess the effectiveness of AONs targeting the PE40 region thereby specifically induce PE40 skipping from *USH2A* pre-mRNA containing the c.7595-2144A>G mutation (**Figure 1c**).

Previous studies demonstrated highest exon-skipping efficiencies using AONs targeting exonic splice enhancer (ESE) motifs recognized by human SRSF2 (SC35), SRSF1 (SF2/ASF) and SRSF5, instead of intron-exon boundaries or other types of splice enhancers.[31,32] Hence, AONs have been designed (sequences in **Table 1**) encompassing most predicted SRSF2, SRSF1, and SRSF5 ESE sequence motifs. AON1 targets five predicted SRSF1, two SRSF2, five SRSF5, and two hexamer ESE sequences, while AON2 targets two SRSF2 and one SRSF5 motifs (**Supplementary Figure S1**). Guidelines for AON design further dictate that AONs should target partially open and partially closed pre-mRNA structures, which is the case for both AON1 (10 closed and 13 open nucleotides) and AON2 (13 closed and 7 open nucleotides). Thermodynamic criteria for AON design include a free energy higher than –4 kcal/mol for self-folding, a free energy higher than –15 kcal/mol for self-dimerisation and a preferable binding energy higher than 20 kcal/mol.[33] All these criteria were met in the design of both AON1 and 2 (**Table 1**).

Fibroblasts from an USH2 patient, having the *USH2A* c.7595-2144A>G (p.Lys2532Thrfs*56) and c.10636G>A (p.Gly3546Arg) mutations in compound heterozygosity, were obtained in order to evaluate the splice correction potential of both AONs. In order to be able to detect PE40-containing *USH2A* transcripts, NMD inhibition using cycloheximide was needed (**Supplementary Figure S2**). Unexpectedly, without NMD inhibition also the *USH2A* allele containing the c.10636G>A (p.Gly3546Arg) missense mutation could not be amplified. This could be the result of quantity-associated detection problems or alternatively could be because the missense variant has an effect on splicing, resulting in an out of frame transcript that is subjected to NMD. However, after NMD inhibition, the presence of this mutation could be confirmed by sequence analysis whereas no indications for alternative splice events were obtained. Subsequent quantitative RT-PCR analyses revealed that the relative *USH2A* transcript levels in the patient-derived and control fibroblasts were 0.12 ± 0.05 and 0.10 ± 0.03% as compared to the expression levels of the housekeeping gene *GUSB*, respectively. Because of the extremely low expression levels in fibroblasts, *USH2A* could only be detected after using a highly sensitive reverse transcriptase, as was already reported by others.[27]

USH2A transcripts from patient-derived fibroblasts were analyzed by RT-PCR using primers in exon 39 (forward) and exon 42 (reverse) which revealed the inclusion of PE40 in mature *USH2A* mRNA (**Figure 2a**), as expected. Transfection of these fibroblasts with either AON1, AON2 or with a cocktail of AON1+2 together in a final concentration of 0.5 µmol/l, resulted in a significant skipping of PE40 (**Figure 2a**), whereas no aberrant splice events were observed when transfecting these AONs in control fibroblasts (**Figure 2a**). RT-qPCR analyses showed that the total amount of *USH2A* transcripts was not significantly altered in AON-treated cells as compared to SON2-treated cells (AON1: P = 0.0797; AON2: P = 0.2039; AON1+2: P = 0.6491 (two-tailed Student's t-test); **Supplementary Figure S3**), which indicates that the PE40-containing transcript is not degraded but instead is converted into the wild-type transcript as a consequence of AON-treatment. We next calculated the relative amount of PE40 incorporation into the *USH2A* transcript by comparing PCR fragment intensities on gel. The ratio of PE40 incorporation was calculated for every PCR product. Around half of the *USH2A* transcripts from untransfected patient fibroblasts contained PE40 (0.56 ± 0.03 (ratio ± SEM) (**Figure 2b**). We observed a minimal difference in the average ratio of PE40 incorporation between untransfected cells and cells transfected with a nonbinding sense oligonucleotide (SON2; 0.44 ± 0.04) (P = 0.0216) (**Figure 2b**), which might be explained by natural variation as a consequence of low *USH2A* transcript levels. Patient fibroblasts transfected with either AON1 or AON2 separately (1 µmol/l), showed a significantly lower average ratio of PE40 incorporation (0.15 ± 0.03; P < 0.0001 and 0.23 ± 0.04; P < 0.01, respectively) as compared to SON2 (**Figure 2b**). Cotransfecting AON1+2 in a 1:1 ratio with the same final concentration of 1 µmol/l resulted in the nearly complete exclusion of PE40 (0.08 ± 0.02; P < 0.0001 when compared to SON2) (**Figure 2b**). AONs 1 and 2 thus both showed the ability to induce skipping of PE40 in patient-derived fibroblasts, however the highest degree of splice correction was induced using a cocktail of AON1+2.

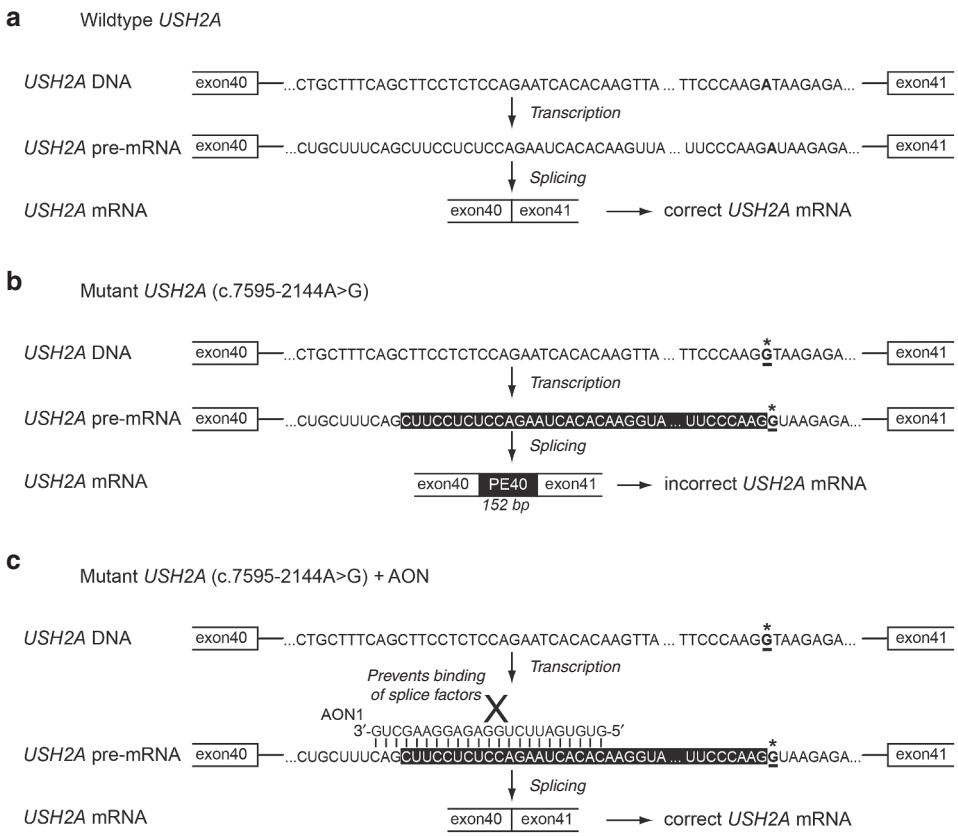

Figure 1 *USH2A* splicing and principle of AON-based splice correction. (**a**) In wild-type alleles, *USH2A* exons 40 and 41 are recognized and fused during splicing of *USH2A* pre-mRNA. (**b**) In case the c.7595-2144A>G mutation is present (indicated with an asterisk), a high-quality splice donor site is created. As a result, the 152 bp directly upstream are recognized as a pseudoexon and incorporated into *USH2A* mRNA (highlighted with a black background). (**c**) Addition of AONs complementary to PE40 can potentially prevent binding of splice factors to that region (indicated by a cross), thereby excluding PE40 from the mature *USH2A* transcript.

Table 1 Sequences and thermodynamic properties of designed 2'-O- methylphosphorothioate AONs

Name	Sequence	Structure (kcal/mol)	Self-dimerisation (kcal/mol)	AON+target (kcal/mol)
AON1	5'-GUGUGAUUCUGGAGAGGAAGCUG-3'	–1.9	–7.6	41.8
AON2	5'-CCCUUAAAAGCCAGCAUACA-3'	1.7	–5.0	30.1
SON2	5'-UGUAUGCUGGCUUUUAAGGG-3'	NA	NA	NA

AON, antisense oligonucleotide; NA, not applicable.

Quantification of the splice redirection potential of the AONs using RT-qPCR analyses appeared to be technically challenging as a result of very low *USH2A* expression levels in fibroblasts, especially in the case of compound heterozygous mutations. For this reason, we set up an *in vitro* minigene splice assay, based on the pCI-NEO plasmid (**Figure 3a**).[34] The genomic region of *USH2A* PE40 (both wild-type and mutant), surrounded by 722 bp up- and 636 bp downstream sequence, was cloned between *RHO* exons 3 and 5 to model splice defects as seen in *USH2A* patients with the c.7595-2144A>G mutation. Indeed, as a consequence of the mutation,[24,26] the mutant minigene splice assay only yielded a transcript consisting of *RHO* exon 3-*USH2A* PE40-*RHO* exon 5 whereas the wild-type minigene splice assay only resulted in a transcript containing *RHO* exons 3 and 5 (**Figure 3b**).

Using an *USH2A* PE40 minigene splice assay, we tried to induce PE40-skipping from the artificial RNA using the same AONs as used to transfect fibroblasts. Cotransfection of the PE40 mutant minigene (1 µg) with 0.5 µmol/l of either AON1 or AON2, resulted in both cases in a combination of corrected and non-corrected transcripts (**Figure 3b**; 274 bp (corrected) versus 426 bp (noncorrected). Subsequent sequence analysis of the noncorrected PCR product derived from AON1-treated samples revealed that the first 12 bp of PE40 were lacking as a consequence of a second cryptic splice acceptor site use. This was neither observed in patient-derived fibroblasts treated with AON1 nor in AON2-treated samples. In addition, the AON1-treated minigene splice assay displayed a faint intermediate splice product, most probably resulting from partially skipped PE40 (**Figure 3b**). Sequence analysis of the lower, presumably corrected fragment, showed that it indeed represents correct splicing of *RHO* exon 3 to exon 5. To exclude AON-induced effects on PE40 splicing independent of the targeted sequence, we reversed the sequence of AON2

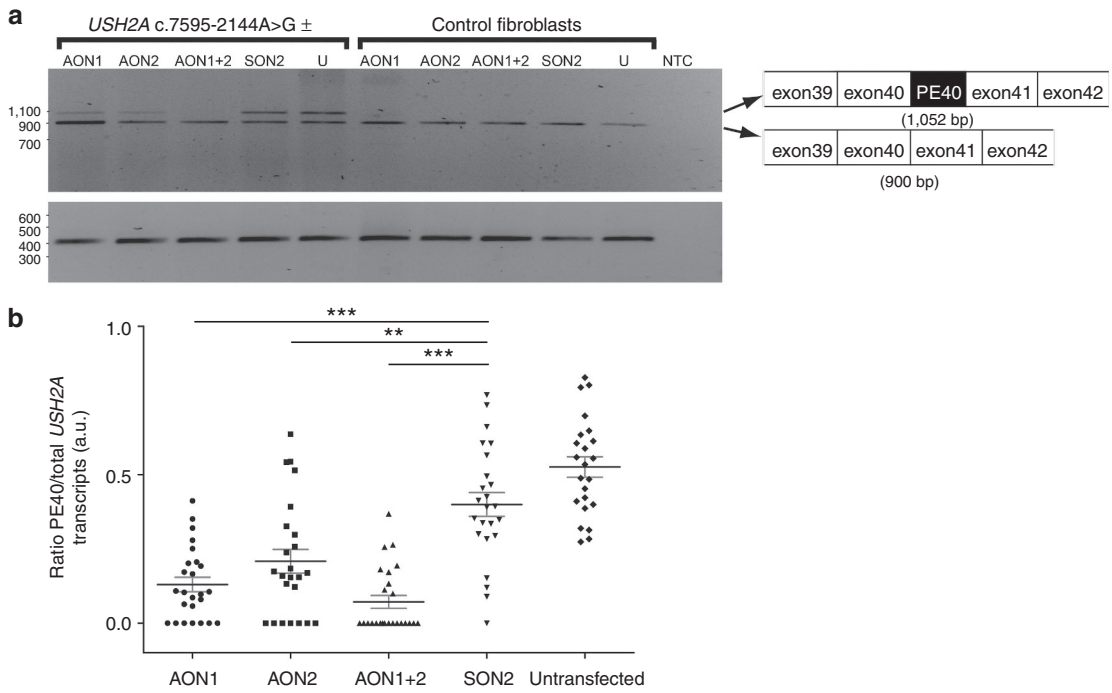

Figure 2 AON-based splice correction in patient-derived fibroblasts. (**a**) One representative sample of each AON treatment is shown, both for patient-derived and control fibroblasts (upper panel). The upper band represents *USH2A* containing PE40, whereas the lower band is *USH2A* lacking PE40. *ACTB* amplification is shown as a loading control (lower panel). (**b**) For every PCR analysis the PE40/(PE40+*USH2A* lacking PE40) transcript ratio was calculated from the gel intensities of PCR products normalized for their fragment length and plotted as a dot, with the mean ratio represented by a horizontal line. Samples in which the *USH2A* transcript lacking PE40 was not amplified were excluded from calculations, which was the case for four datapoints (one in both AON2 and SON2 and two in the non-AON treated cells). An unpaired two-tailed Student's *t*-test was used to compare calculated ratios between AON-treated and SON-treated patient-derived fibroblasts, showing a significant reduction of PE40 incorporation in all three AON treatment (AON1, AON2, and AON1+2) conditions (indicated by ***($P < 0.001$) or **($P < 0.01$)). Grey error bars: SEM; NTC: negative template control; U: untreated control; a.u.: arbitrary units.

into a sense orientation (SON2). Cotransfecting the PE40 mutant minigene splice assay with the nonbinding SON2 did not result in splice modulation of PE40, demonstrating the specificity of the result obtained with the antisense sequences (**Figure 3c**). These results were in total agreement with the results obtained from AON-treated patient-derived fibroblasts (**Figure 2a**,**b**). Since both AONs 1 and 2 showed exon-skipping potential using the minigene splice assay, we next lowered AON concentrations ranging from 1.0 to 0.01 µmol/l in order to determine the minimal concentration at which the AONs were still able to induce significant PE40 splice redirection. As shown in **Figure 4a**,**b**, for both AON1 and AON2, we observed a gradual decrease of PE40-containing transcripts to coincide with increasing concentrations of AON. When cotransfecting AON1 and 2 as a cocktail, a similar PE40-skipping effect was seen (**Figure 4c**). However, in contrast to what we observed for both AON1 and 2 individually, a steep turning point in splice redirection potential was seen between a total AON concentration of 0.1 and 0.05 µmol/l. In addition, we observed a decrease in target transcripts when applying AON1 at higher concentrations (0.5 or 1 µmol/l) to our minigene splice assay (**Figure 4a**), which we attributed as the result of toxicity.

In conclusion, we were able to show that designed AONs are able to induce PE40-skipping in both patient-derived fibroblasts and *in vitro* minigene splice assays.

Discussion

Mutations in *USH2A* that affect splicing are responsible for Usher syndrome type 2 and autosomal recessive retinitis pigmentosa. Recent identification of four deep-intronic mutations leading to inclusion of PEs underlines the importance of this pathogenic mechanism,[24,25] that was underestimated a few years ago. In this work, we used the c.7595-2144A>G mutation, which represents the second most frequent *USH2A* mutation in some populations, as a model to initiate the development of an AON-based therapy for *USH2A*-associated retinitis pigmentosa.

Mutations that affect pre-mRNA splicing represent a significant fraction of disease-causing mutations, in a variety of inherited disorders.[35,36] Different strategies have been employed to correct the resulting splice defects, of which AON treatment seems most promising. AONs do not alter endogenous transcription levels and also their relative ease in design and low production costs can be regarded favorable for AON-based therapies.[35,37] The sequence-specific properties of AONs make them suitable for interfering with splicing processes for different therapeutic purposes.[38,39] Next to skipping of (pseudo)exons, AONs have been shown to be able to retain exons that are skipped as a consequence of splice site mutations.[40,41] In addition, AONs can be used to alter the ratio between two naturally occurring alternatively spliced transcripts.[38]

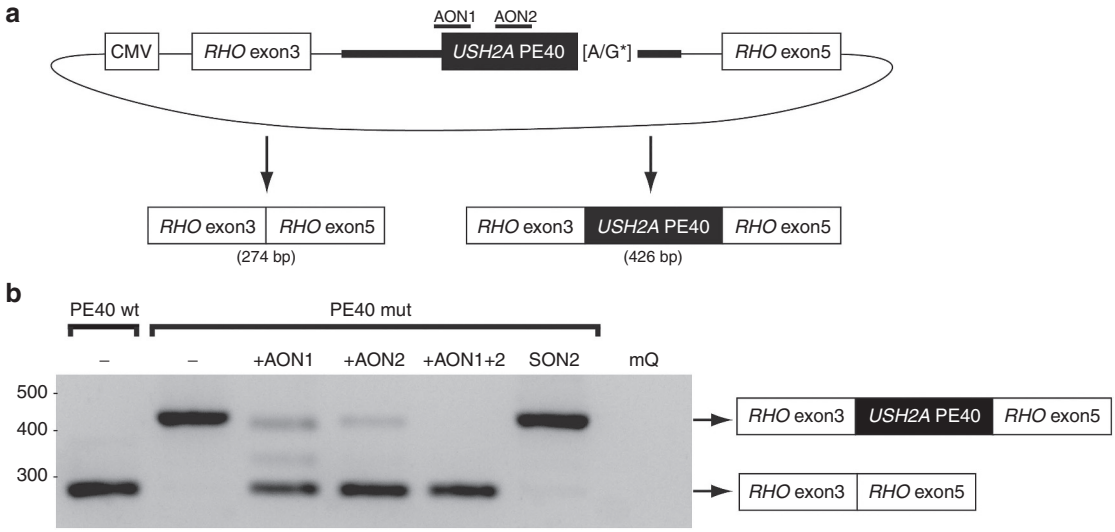

Figure 3 *USH2A* PE40 minigene splice assay to assess AON efficacy *in vitro*. (**a**) Schematic representation of the minigene splice assay, with the nucleotide corresponding to the *USH2A* c.7595-2144A>G substitution highlighted with an asterisk. The genomic *USH2A* PE40 sequence (indicated with a black background "*USH2A* PE40") and flanking sequences (indicated with a fat black line) were cloned between *RHO* exons 3 and 5. Targeting sequence of AON1 and AON2 is schematically indicated above the *USH2A* PE40 region. (**b**) RT-PCR analysis of *RHO* ex3-*USH2A* PE40 wild-type/mutant-*RHO* ex5 RNAs, isolated from transfected HEK293T cells that were cultured in the absence or presence of AON1, AON2, or AON1 and 2 together. AONs are directed against the aberrant *USH2A* PE40 exon and used in a final concentration of 0.5 µmol/l. The upper bands represent the aberrant *RHO-USH2A* PE40 splice product (426 or 414 bp when AON1-treated), whereas the lower bands represent the corrected transcript without *USH2A* PE40 (274 bp). Also an intermediate splice product was observed after AON1 treatment. SON2 is a nonbinding control sense oligonucleotide and cotransfection into HEK293T cells with the minigene splice assay only gives rise to the aberrant splice product. Water (mQ) was used as a negative control.

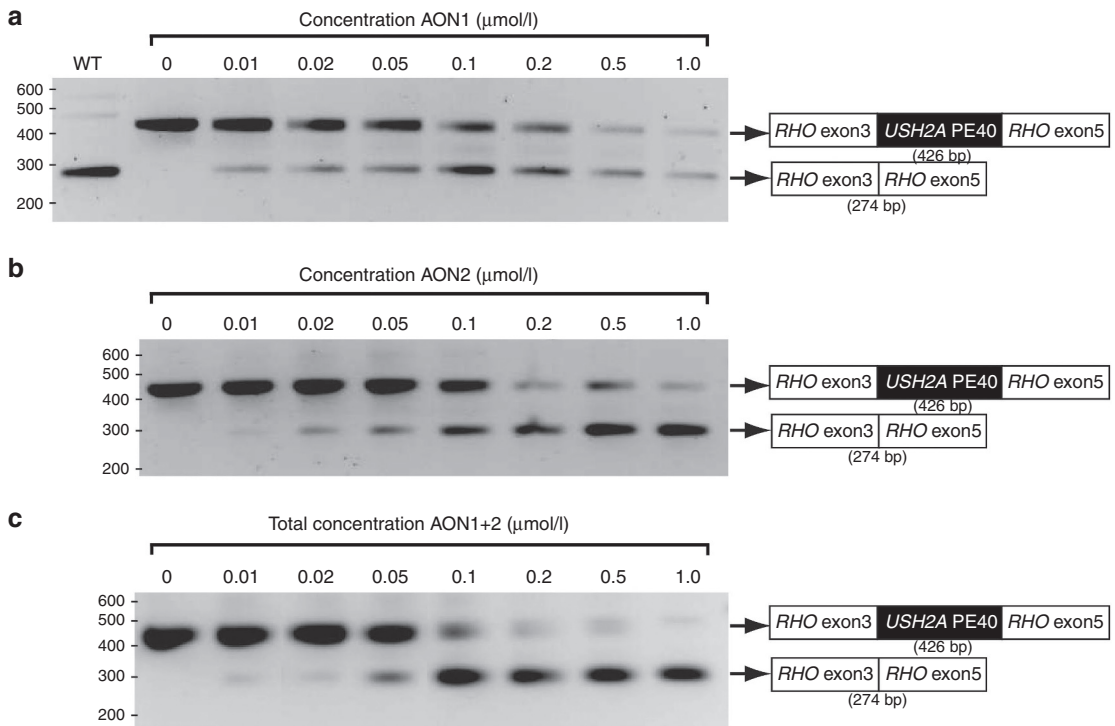

Figure 4 Dose-dependent AON-induced splice correction of *USH2A* using a minigene splice assay. RT-PCR analysis of *RHO* ex3-*USH2A* PE40 mutant-*RHO* ex5 transcripts isolated from transfected HEK293T cells that were cultured in the absence or presence of different end-concentrations of AON1 (**a**), AON2 (**b**), or AON1+2 (**c**), ranging from 0 to 1.0 µmol/l. PCR (30 cycles) was performed from *RHO* exon 3 to exon 5, in order to specifically amplify minigene splice assay derived cDNA. The lower band (274 bp) represents the transcript without *USH2A* PE40.

Several preclinical proof-of-concept studies for AON-based RNA splice modulation therapy have been performed, showing promising results for different genetic disorders such as Leber congenital amaurosis, Hutchinson-Gilford progeria syndrome, spinal muscular atrophy or Duchenne muscular dystrophy.[31,42–48] As a consequence, AONs are now in or beyond different phase 1, 2, or 3 clinical trials to evaluate their therapeutic potential and biosafety.[49–51] No major adverse effects have been observed in patients with Duchenne muscular dystrophy after subcutaneous injections with Drisapersen, however mild-to-moderate reactions at the site of injection and proteinuria have been observed in most cases.[52] Increasing doses of Drisapersen above 6 mg/kg are less well tolerated and lead to inflammatory responses.[53] The phosphorothioate backbone can be immunostimulatory mainly via the nucleic acid recognizing toll like receptors (TLRs) 3, 7, 8 and 9 (ref. 54). Although not proven, direct delivery into the eye will most probably circumvent systemic exposure of AONs to TLRs due to the presence of a blood-retinal barrier, however, *TLR3* expression has also been observed in retinal pigment epithelium cells.[55] 2'-O-methyl modification of the riboses within the phosphorothioate backbone has been described to prevent activation of TLR7-9, but not of TLR3 (ref. 56). As TLR3 recognizes double stranded DNA,[56] it is not expected that a TLR3-activated inflammatory response will be induced upon an intraocular delivery of AONs.[57]

Different guidelines to aid AON design have been described by others.[33,37] AONs complementary to exonic splice enhancer (ESE) motifs that are targeted by Ser-Arg-rich splice modulators, in particular SRSF1 (SF2/ASF), SRSF2 (formerly known as SC35) and SRSF5, have been shown to be most effective in exon skipping.[37] Also, it has been shown that effective AONs often bind close to the splice acceptor site and the free energy of the AON-target complex is higher than that of the target complex and that of the AON individually.[37] By adopting these guidelines we have designed two different AONs and examined the exon-skipping potential after single AON addition or after addition of a cocktail consisting of the two AONs. AON1 has been designed to target five predicted SRSF1, two SRSF2, five SRSF5, and two hexamer ESE sequence motifs, thereby overlapping the PE40 splice acceptor site. The use of AON1 in combination with a minigene splice assay results in the use of an alternative splice acceptor site 12 bp downstream of the regular PE40 splice acceptor site. Although this effect has not been observed in fibroblasts treated with AON1 and/or AON2, we cannot rule out that, due to the low level of *USH2A* expression, we are unable to detect any alternatively spliced transcripts. In line with other studies, suggesting that the use of a cocktail of AONs is often more potent than using a single AON,[58–60] our results show that a combination of AON1+2 is indeed more potent than using either AON individually.

In our study, we show *USH2A* splice correction in biologically nonrelevant patient-derived fibroblasts and minigene splice assays. However, this does not result in the production of functional USH2A protein. In order to evaluate the effect of AON-induced splice correction on the level of photoreceptor maintenance and function, physiological relevant cellular and/or animal models will be crucial. Using iPSC technology, it is possible to generate photoreceptor-like cells from patient-derived keratinocytes or fibroblasts, which has already been shown for an *USH2A* patient having the c.7595-2144A>G mutation in compound heterozygosity with the c.12575G>A; p.Arg4192His mutation.[26] The use of photoreceptor-like cells will enable the assessment of potential AON-induced off-target effects by sequencing total RNA from those artificial eyecups. For the evaluation of visual function, animal models will be essential. However, the currently available *Ush2a* knockout mouse model only shows a mild retinal degeneration with a very late age of onset.[61] Zebrafish can be an attractive alternative model for studying Usher syndrome-related retinal degeneration.[62] Electroretinogram (ERG) traces have been shown to be significantly attenuated in zebrafish *Myo7a* (USH1b), *Ush1c* (USH1c), and *Pcdh15b* (USH1f) mutants and morphants.[63–65] In addition, morpholino-induced knockdown of zebrafish *Ush2a* results in moderate levels of early-onset photoreceptor degeneration in larvae (5 days postfertilization).[66] Although the effect of human mutations on splicing is not always recapitulated in non-human species,[67] the c.7595-2144A>G mutation results in a consensus ("GTAAG") splice donor site. Recent advances in CRISPR/Cas9 technology now enable the generation of a humanized locus for the *USH2A* PE40 intronic sequence in zebrafish. Future research will determine whether the effect of the c.7595-2144A>G mutation is recapitulated in a humanized zebrafish, and whether this model will be suitable to evaluate the effect of AON-induced splice correction on the level of visual function.

Once an animal model is present, the next challenge will be the delivery of AONs to photoreceptor cells. Systemic drug administration is one possible route for treating retinal disorders. However, retinal transfer of drugs from the circulating blood is strictly regulated by two blood–ocular barrier systems, the blood–aqueous barrier and the blood-retinal barrier.[45,68,69] In order to effectively overcome these physical barriers, AONs need to be delivered directly into the human eye, either via injections of naked AONs into the vitreous humor or by using a stabilizing vehicle (*e.g.*, recombinant virus, designed nanoparticles, cell penetrating peptides, exosomes, or liposomes).[35,70,71] Once present in the eye, naked AONs have proven to be able to freely diffuse into all cells of the retina to interfere with splicing.[45] When using naked AONs, it will be needed to repeatedly supplement photoreceptor cells with AONs, since effectiveness will be lost over time due to AON degradation or wash out. Intravitreal injections in mice have demonstrated that 2'-O-methylphosphorothioate AONs are effective in photoreceptor cells for at least 1 month and probably longer.[45] Therefore, we speculate that patients will need a few intravitreal AON administrations per year.

A durable splice correction effect is likely to be achieved by administration of an AAV vector expressing AON sequences linked to a modified U7 small nuclear RNA (U7 snRNA). Via this route, it will be possible to induce the same therapeutic effect as with naked AONs, but presumably with a long-lasting effect.[72–74] However, traditionally AAVs are unable to cross the retinal layers from vitreous humor into photoreceptor cells due to the presence of a diffusive barrier made up by the inner limiting membrane.[75] In addition, also the presence of neutralizing antibodies may reduce successful photoreceptor

infection from intravitreally injected AAVs.[76] For this reason, AAVs will need to be injected subretinally, limiting the targeted retinal area.[77] However, a recent study presented a promising rAAV serotype which can be efficiently delivered intravitreally.[78] After transduction, the rAAV DNA strands will form very stable episomal structures, from which transcription can take place. Since photoreceptor cells are nondividing cells, integration in their genome is not a pre-requisite for success and therefore the use of rAAVs instead of integrating (retro)viruses will lower the risk of potential side effects without reducing AON effectiveness.

Besides presenting with retinal degeneration, Usher syndrome patients suffer from congenital hearing impairment. Usher proteins have been shown to be the structural components of the fibrous links between hair cell stereocilia and essential for proper hair bundle formation and function (reviewed by Kremer *et al.*[79]). *USH1C* encodes harmonin, a protein directly connected to the USH2A protein in both hair cells and photoreceptors.[80] Treatment of an *Ush1c* mouse model with splice modulating AONs anytime during the first thirteen days after birth, results in a restored orientation and function of cochlear hair bundles.[81] Treatment on this mouse from post-natal day 16 onwards, which corresponds to 5 months of gestation in humans, shows no beneficial effects anymore. Therefore, AON-based splice correction will probably only be effective when administered during or prior to the development of inner ear hair bundles.

In conclusion, this study shows that administration of engineered AONs to fibroblasts of an individual affected by Usher syndrome almost fully restores a splice defect that is caused by the frequent deep-intronic c.7595-2144A>G mutation in *USH2A*. Although promising on transcript level, future research is needed to determine the therapeutic potential of AON-based splice correction as a treatment to stop or slowdown the progression of this devastating blinding aspect of Usher syndrome and isolated *USH2A*-associated retinitis pigmentosa.

Materials and methods

Antisense oligonucleotides. The sequence of *USH2A* PE40 was analyzed for the presence of exonic splice enhancer motifs using the online ESE finder 3.0 program (http://rulai.cshl.edu/cgi-bin/tools/ESE3/esefinder.cgi?process=home) with standard settings. The presence of RESCUE-ESE sites was determined using the RESCUE-ESE tool (http://genes.mit.edu/burgelab/rescue-ese/). AONs were subsequently designed to each cover multiple SRSF1, SRSF2, SRSF5, or hexamers in PE40. Furthermore, the energetically most stable secondary structure of *USH2A* PE40 (including 25 nucleotides of flanking sequence both up- and downstream) was predicted using the RNAStructure software (http://rna.urmc.rochester.edu/rnastructure.html).[82] In addition, we picked sequences to be targeted by AONs predicted as "partially open". With the same webtool, also thermodynamic criteria were evaluated: free energy of the AON, of the AON-AON complexes and of binding energy between the AON and its target sequence.[33] AONs according above criteria were designed with a T_m of 58 °C and a GC% between 40–60%. The uniqueness of the AON target sequences was determined by BLAST analysis. The two most optimal AONs were purchased from Eurogentec (Liège, Belgium) containing 2'-O-methyl modified riboses and a phosphorothioate backbone (sequences are presented in **Table 1**). As a nonbinding control, a sense orientation of AON2 was also acquired (named SON2). AONs were dissolved in phosphate-buffered saline (PBS) before use.

USH2A qPCR analysis. Total RNA was isolated from fibroblasts using the Nucleospin RNA II isolation kit (MACHEREY-NAGEL #740955.50, Düren, Germany), according to manufacturer's protocol. Subsequently, 0.5–1.0 µg of total RNA was used for cDNA synthesis with SuperScript III RT (Life Technologies, #11755050, Carlsbad, CA). *USH2A* was subsequently amplified using forward primer 5'-CCAGGGAAAAGAGCAGAGTG-'3 (exon 28) and reverse primer 5'-GATAGCCTCGCATGAAGGAG-3' (exon 29). The housekeeping gene *GUSB* was used as a reference using the forward primer 5'-AGAGTGGTGCTGAGGATTGG-'3 (exon 2) and reverse primer 5'-GACACGCTAGAGCATGAGGG-3' (exon 3). GoTaq (Promega A6001) was used to amplify *USH2A* and *GUSB* cDNA in triplicate in a 7500 HT qPCR machine. Analysis of the qPCR data was performed with 7500 software (version 2.3), with the CT-threshold set manually. Subsequently, *USH2A*/*GUSB* ratios were calculated to obtain relative *USH2A* transcript levels.

Minigene splice assays. A plasmid containing the genomic region of *RHO* encompassing exons 3–5 inserted at the EcoRI/SalI sites in the pCI-NEO vector[34] was adapted to the Gateway cloning system, as previously described.[83] Using Gateway cloning technology, human *USH2A* PE40 (wild-type and mutant) together with 722 bp of 5'-flanking and 636 bp of 3'-flanking intronic sequence was inserted in the vector.

Cell culture. HEK293T cells were cultured in Dulbecco's modified Eagle's medium (DMEM)(Sigma-Aldrich D0819, St. Louis, MO) supplemented with 10% (v/v) fetal bovine serum (Sigma-Aldrich F7524) and 1% penicillin-streptomycin (Sigma-Aldrich P4333). Cells were passaged twice a week. Primary fibroblasts of an USH2 patient, with compound heterozygous *USH2A* mutations (c.7595-2144A>G and c.10636G>A), were cultured in DMEM (Sigma-Aldrich D0819) supplemented with 20% fetal bovine serum (Sigma-Aldrich F7524), 1% sodium pyruvate (Sigma-Aldrich S8636) and 1% penicillin-streptomycin (Sigma-Aldrich P4333). Cells were passaged twice a week.

Transfection of AONs in patient-derived fibroblasts. Fibroblasts were seeded at a concentration of 5.0×10^5 cells/well in a 12-well plate. Cells were subsequently transfected with AONs using FuGENE HD Transfection Reagent (Promega, #E2311, Madison, WI) according to manufacturer's instructions, in quintuplicate. Twenty-four hours after transfection, cells were treated for an additional 16 hours with cycloheximide (Sigma-Aldrich, #C4859—final concentration of 100 µg/ml in DMEM medium with all supplements as described before) prior to RNA isolation in order to inhibit nonsense-mediated decay of the *USH2A* PE40-containing transcripts.

Transfection of AONs and minigene splice assay in HEK293T cells. One day before transfection, 5.0×10^5 HEK293T cells were seeded in each well of a 12-well plate, in a total volume of 0.9 ml medium containing all supplements as described before. Transfection mixtures were prepared by combining 1 µl AON in a desired concentration as indicated in the graphs, 500 ng of plasmid DNA and 45 µl polyethylenimine transfection reagent (PEI). Mixtures were incubated at room temperature for 10 minutes, before being dropwise added to the cells. Forty-eight hours after transfection, cells were collected using a cell scraper and washed with 1x PBS prior to RNA isolation.

RNA isolation and RT-PCR. Total RNA was isolated from transfected HEK293T or fibroblasts using the Nucleospin RNA II isolation kit (MACHEREY-NAGEL #740955.50, Düren, Germany), according to manufacturer's protocol. Subsequently, 0.5–1.0 µg of total RNA was used for cDNA synthesis with iScript cDNA synthesis kit (Bio-Rad, #170–8891) or SuperScript III RT (Life Technologies, #11755050) for HEK293T and primary fibroblasts respectively. For the splice correction experiments with the minigene splice assay, part of the cDNA was amplified under standard PCR conditions using Q5 polymerase (New England Biolabs, #M0491L, Ipswich, MA) and using forward primer 5'-CGGAGGTCAACAACGAGTCT-3' and reverse primer 5'-AGGTGTAGGGGATGGGAGAC-3' that are designed for exons 3 and 5 of the human *RHO* gene, respectively. For the splice correction experiments in fibroblasts, part of the *USH2A* cDNA was amplified under standard PCR conditions using Q5 polymerase and the primers 5'-GCTCTCCCAGATACCAACTCC-3' and 5'-GATTCACATGCCTGACCCTC-3' designed for exons 39 and 42, respectively. A PCR amplifying *ACTB* cDNA using forward primer 5'-ACTGGGACGACATGGAGAAG-3' and reverse primer 5'-CTTCACCACCACAGCTGAGA-3' was employed as a control for the amount of lysed cell material. Every cDNA sample was analysed in quintuplicate, yielding in total 25 datapoints per AON. PCR products were separated on a 1.5% agarose gel. Fragments presumably representing correctly and aberrantly spliced *USH2A* were excised from the gel, purified using Nucleospin Extract II isolation kit (MACHEREY-NAGEL, #740609.250) and sequenced from both strands with the ABIPRISM Big Dye Terminator Cycle Sequencing V2.0 Ready Reaction kit and the ABIPRISM 3730 DNA analyzer (Applied Biosystems, Foster City, CA).

Quantification of PCR product intensities and ratio calculation. PCR products were size separated on a 1% agarose gel, and DNA was visualized using ethidium bromide. Gels were photographed with an Isogen Life sciences imager using ProXima AQ-4 (v3.0) software and subsequently quantified with ImageJ (v1.46r) software. Both PE40-containing fragments and *USH2A* fragments lacking PE40 were covered in a square with an equal surface area, from which the intensity profile was subsequently generated. The peaks' bases were closed manually by drawing a horizontal line, after which the surface of the peaks was calculated, representing *USH2A* PE40-containing transcripts and transcripts lacking PE40. These values were transferred to Microsoft Excel 2007 and normalized for their product size (*i.e.*, 1,052 or 900 bp). The total amount of *USH2A* transcripts (*i.e.*, the sum of PE40-containing and PE40-lacking band intensities) and the PE40 transcript ratio (*i.e.*, PE40-containing transcripts divided by total *USH2A* transcripts) was calculated per condition. Samples in which the *USH2A* transcript lacking PE40 was not amplified were excluded from calculations, which was the case for four PCR products (one in both AON2 and SON2 and two samples in the non-AON-treated cells). Each gel image was analyzed twice, from which the average was plotted in a dot-plot using GraphPad Prism (v5.03, GraphPad Software, San Diego, CA). Statistical analyses were subsequently performed with a two-tailed unpaired Student's *t*-test using GraphPad Prism.

Supplementary material

Figure S1. Predicted ESE sequence motifs in *USH2A* PE40.
Figure S2. Cycloheximide treatment induces stabilization of PE40 containing transcripts.
Figure S3. Quantification of total *USH2A* transcript level after AON treatment of fibroblasts.

Acknowledgments The authors would like to thank the CIBERER biobank (Valencia, Spain) for sharing *USH2A* patient-derived primary fibroblasts. This work is financially supported by the Dutch Organisation for Scientific research (NWO Veni grant 016.136.091; E.V.W.), the Dutch Organisation for Health Research and Development (ZonMW E-rare grant "Eur-USH" 40-42900-98-1006; E.V.W.), the Dutch eye foundations (Stichting Nederlands Oogheelkundig Onderzoek, SAFDOR and Stichting Blindenhulp; E.V.W. and H.K.), the French national union of blind and visually impaired people (UNADEV; A-FR), and the French National Research Agency (E-rare grant "Eur-USH" ANR-12-RARE-006-03; CV). The work in this manuscript has been patented under number PCT/EP2015/065736. E.V.W. reports being employed by Radboudumc and inventor on this patent. Radboudumc has licensed the rights to the patent exclusively to ProQR Therapeutics. As the inventor, E.V.W. is entitled to a share of any future royalties paid to Radboudumc, should the therapy eventually be brought to the market.

1. Kimberling, WJ, Hildebrand, MS, Shearer, AE, Jensen, ML, Halder, JA, Trzupek, K *et al.* (2010). Frequency of Usher syndrome in two pediatric populations: Implications for genetic screening of deaf and hard of hearing children. *Genet Med* **12**: 512–516.
2. Millán, JM, Aller, E, Jaijo, T, Blanco-Kelly, F, Gimenez-Pardo, A and Ayuso, C (2011). An update on the genetics of usher syndrome. *J Ophthalmol* **2011**: 417217.
3. Yan, D and Liu, XZ (2010). Genetics and pathological mechanisms of Usher syndrome. *J Hum Genet* **55**: 327–335.
4. Sadeghi, AM, Cohn, ES, Kimberling, WJ, Halvarsson, G and Möller, C (2013). Expressivity of hearing loss in cases with Usher syndrome type IIA. *Int J Audiol* **52**: 832–837.
5. Hartong, DT, Berson, EL and Dryja, TP (2006). Retinitis pigmentosa. *Lancet* **368**: 1795–1809.
6. Seyedahmadi, BJ, Rivolta, C, Keene, JA, Berson, EL and Dryja, TP (2004). Comprehensive screening of the USH2A gene in Usher syndrome type II and non-syndromic recessive retinitis pigmentosa. *Exp Eye Res* **79**: 167–173.
7. McGee, TL, Seyedahmadi, BJ, Sweeney, MO, Dryja, TP and Berson, EL (2010). Novel mutations in the long isoform of the USH2A gene in patients with Usher syndrome type II or non-syndromic retinitis pigmentosa. *J Med Genet* **47**: 499–506.
8. Blanco-Kelly, F, Jaijo, T, Aller, E, Avila-Fernandez, A, López-Molina, MI, Giménez, A *et al.* (2015). Clinical aspects of Usher syndrome and the USH2A gene in a cohort of 433 patients. *JAMA Ophthalmol* **133**: 157–164.
9. Sandberg, MA, Rosner, B, Weigel-DiFranco, C, McGee, TL, Dryja, TP and Berson, EL (2008). Disease course in patients with autosomal recessive retinitis pigmentosa due to the USH2A gene. *Invest Ophthalmol Vis Sci* **49**: 5532–5539.

10. Pierrache, LH, Hartel, BP, van Wijk, E, Meester-Smoor, MA, Cremers, FP, de Baere, E *et al.* (2016). Visual prognosis in USH2A-associated retinitis pigmentosa is worse for patients with Usher syndrome type IIa than for those with nonsyndromic Retinitis Pigmentosa. *Ophthalmology* **123**: 1151–1160.
11. Hashimoto, T, Gibbs, D, Lillo, C, Azarian, SM, Legacki, E, Zhang, XM *et al.* (2007). Lentiviral gene replacement therapy of retinas in a mouse model for Usher syndrome type 1B. *Gene Ther* **14**: 584–594.
12. Lopes, VS, Boye, SE, Louie, CM, Boye, S, Dyka, F, Chiodo, V *et al.* (2013). Retinal gene therapy with a large MYO7A cDNA using adeno-associated virus. *Gene Ther* **20**: 824–833.
13. Colella, P, Trapani, I, Cesi, G, Sommella, A, Manfredi, A, Puppo, A *et al.* (2014). Efficient gene delivery to the cone-enriched pig retina by dual AAV vectors. *Gene Ther* **21**: 450–456.
14. Zallocchi, M, Binley, K, Lad, Y, Ellis, S, Widdowson, P, Iqball, S *et al.* (2014). EIAV-based retinal gene therapy in the shaker1 mouse model for usher syndrome type 1B: development of UshStat. *PLoS One* **9**: e94272.
15. Bainbridge, JW, Smith, AJ, Barker, SS, Robbie, S, Henderson, R, Balaggan, K *et al.* (2008). Effect of gene therapy on visual function in Leber's congenital amaurosis. *N Engl J Med* **358**: 2231–2239.
16. Cideciyan, AV, Aleman, TS, Boye, SL, Schwartz, SB, Kaushal, S, Roman, AJ *et al.* (2008). Human gene therapy for RPE65 isomerase deficiency activates the retinoid cycle of vision but with slow rod kinetics. *Proceed Natl Acad Sci USA* **105**, 15112–15117.
17. Hauswirth, WW, Aleman, TS, Kaushal, S, Cideciyan, AV, Schwartz, SB, Wang, L *et al.* (2008). Treatment of leber congenital amaurosis due to RPE65 mutations by ocular subretinal injection of adeno-associated virus gene vector: short-term results of a phase I trial. *Hum Gene Ther* **19**: 979–990.
18. Maguire, AM, Simonelli, F, Pierce, EA, Pugh, EN Jr, Mingozzi, F, Bennicelli, J *et al.* (2008). Safety and efficacy of gene transfer for Leber's congenital amaurosis. *N Engl J Med* **358**: 2240–2248.
19. Savić, N and Schwank, G (2016). Advances in therapeutic CRISPR/Cas9 genome editing. *Transl Res* **168**: 15–21.
20. Roux, AF, Faugère, V, Vaché, C, Baux, D, Besnard, T, Léonard, S *et al.* (2011). Four-year follow-up of diagnostic service in USH1 patients. *Invest Ophthalmol Vis Sci* **52**: 4063–4071.
21. Baux, D, Blanchet, C, Hamel, C, Meunier, I, Larrieu, L, Faugère, V *et al.* (2014). Enrichment of LOVD-USHbases with 152 USH2A genotypes defines an extensive mutational spectrum and highlights missense hotspots. *Hum Mutat* **35**: 1179–1186.
22. Aller, E, Larrieu, L, Jaijo, T, Baux, D, Espinós, C, González-Candelas, F *et al.* (2010). The USH2A c.2299delG mutation: dating its common origin in a Southern European population. *Eur J Hum Genet* **18**: 788–793.
23. Pennings, RJ, Te Brinke, H, Weston, MD, Claassen, A, Orten, DJ, Weekamp, H *et al.* (2004). USH2A mutation analysis in 70 Dutch families with Usher syndrome type II. *Hum Mutat* **24**: 185.
24. Vaché, C, Besnard, T, le Berre, P, García-García, G, Baux, D, Larrieu, L *et al.* (2012). Usher syndrome type 2 caused by activation of an USH2A pseudoexon: implications for diagnosis and therapy. *Hum Mutat* **33**: 104–108.
25. Liquori, A, Vaché, C, Baux, D, Blanchet, C, Hamel, C, Malcolm, S *et al.* (2016). Whole USH2A gene sequencing identifies several new deep intronic mutations. *Hum Mutat* **37**: 184–193.
26. Tucker, BA, Mullins, RF, Streb, LM, Anfinson, K, Eyestone, ME, Kaalberg, E *et al.* (2013). Patient-specific iPSC-derived photoreceptor precursor cells as a means to investigate retinitis pigmentosa. *Elife* **2**: e00824.
27. Steele-Stallard, HB, Le Quesne Stabej, P, Lenassi, E, Luxon, LM, Claustres, M, Roux, AF *et al.* (2013). Screening for duplications, deletions and a common intronic mutation detects 35% of second mutations in patients with USH2A monoallelic mutations on Sanger sequencing. *Orphanet J Rare Dis* **8**: 122.
28. Krawitz, PM, Schiska, D, Krüger, U, Appelt, S, Heinrich, V, Parkhomchuk, D *et al.* (2014). Screening for single nucleotide variants, small indels and exon deletions with a next-generation sequencing based gene panel approach for Usher syndrome. *Mol Genet Genomic Med* **2**: 393–401.
29. Aparisi, MJ, Aller, E, Fuster-García, C, García-García, G, Rodrigo, R, Vázquez-Manrique, RP *et al.* (2014). Targeted next generation sequencing for molecular diagnosis of Usher syndrome. *Orphanet J Rare Dis* **9**: 168.
30. Sodi, A, Mariottini, A, Passerini, I, Murro, V, Tachyla, I, Bianchi, B *et al.* (2014). MYO7A and USH2A gene sequence variants in Italian patients with Usher syndrome. *Mol Vis* **20**: 1717–1731.
31. Collin, RW, den Hollander, AI, van der Velde-Visser, SD, Bennicelli, J, Bennett, J and Cremers, FP (2012). Antisense oligonucleotide (AON)-based therapy for Leber congenital amaurosis caused by a frequent mutation in CEP290. *Mol Ther Nucleic Acids* **1**: e14.
32. Aartsma-Rus, A, Houlleberghs, H, van Deutekom, JC, van Ommen, GJ and 't Hoen, PA (2010). Exonic sequences provide better targets for antisense oligonucleotides than splice site sequences in the modulation of Duchenne muscular dystrophy splicing. *Oligonucleotides* **20**: 69–77.
33. Aartsma-Rus, A (2012). Overview on AON design. *Methods Mol Biol* **867**: 117–129.
34. Gamundi, MJ, Hernan, I, Muntanyola, M, Maseras, M, López-Romero, P, Alvarez, R *et al.* (2008). Transcriptional expression of cis-acting and trans-acting splicing mutations cause autosomal dominant retinitis pigmentosa. *Hum Mutat* **29**: 869–878.
35. Hammond, SM and Wood, MJ (2011). Genetic therapies for RNA mis-splicing diseases. *Trends Genet* **27**: 196–205.
36. Wang, GS and Cooper, TA (2007). Splicing in disease: disruption of the splicing code and the decoding machinery. *Nat Rev Genet* **8**: 749–761.
37. Aartsma-Rus, A, van Vliet, L, Hirschi, M, Janson, AA, Heemskerk, H, de Winter, CL *et al.* (2009). Guidelines for antisense oligonucleotide design and insight into splice-modulating mechanisms. *Mol Ther* **17**: 548–553.
38. Siva, K, Covello, G and Denti, MA (2014). Exon-skipping antisense oligonucleotides to correct missplicing in neurogenetic diseases. *Nucleic Acid Ther* **24**: 69–86.
39. Gerard, X, Garanto, A, Rozet, JM and Collin, RW (2016). Antisense Oligonucleotide Therapy for Inherited Retinal Dystrophies. *Adv Exp Med Biol* **854**: 517–524.
40. Igreja, S, Clarke, LA, Botelho, HM, Marques, L and Amaral, MD (2016). Correction of a Cystic Fibrosis Splicing Mutation by Antisense Oligonucleotides. *Hum Mutat* **37**: 209–215.
41. Skordis, LA, Dunckley, MG, Yue, B, Eperon, IC and Muntoni, F. (2003). Bifunctional antisense oligonucleotides provide a trans-acting splicing enhancer that stimulates SMN2 gene expression in patient fibroblasts. *Proceed Natl Acad Sci USA* **100**, 4114–4119.
42. Scaffidi, P and Misteli, T (2005). Reversal of the cellular phenotype in the premature aging disease Hutchinson-Gilford progeria syndrome. *Nat Med* **11**: 440–445.
43. Cirak, S, Feng, L, Anthony, K, Arechavala-Gomeza, V, Torelli, S, Sewry, C *et al.* (2012). Restoration of the dystrophin-associated glycoprotein complex after exon skipping therapy in Duchenne muscular dystrophy. *Mol Ther* **20**: 462–467.
44. Hua, Y, Sahashi, K, Hung, G, Rigo, F, Passini, MA, Bennett, CF *et al.* (2010). Antisense correction of SMN2 splicing in the CNS rescues necrosis in a type III SMA mouse model. *Genes Dev* **24**: 1634–1644.
45. Gérard, X, Perrault, I, Munnich, A, Kaplan, J and Rozet, JM (2015). Intravitreal injection of splice-switching oligonucleotides to manipulate splicing in retinal cells. *Mol Ther Nucleic Acids* **4**: e250.
46. Garanto, A, Chung, DC, Duijkers, L, Corral-Serrano, JC, Messchaert, M, Xiao, R *et al.* (2016). *In vitro* and *in vivo* rescue of aberrant splicing in CEP290-associated LCA by antisense oligonucleotide delivery. *Hum Mol Genet* (epub ahead of print).
47. Gerard, X, Perrault, I, Hanein, S, Silva, E, Bigot, K, Defoort-Delhemmes, S *et al.* (2012). AON-mediated exon skipping restores ciliation in fibroblasts harboring the common Leber congenital amaurosis CEP290 mutation. *Mol Ther Nucleic Acids* **1**: e29.
48. Parfitt, DA, Lane, A, Ramsden, CM, Carr, AJ, Munro, PM, Jovanovic, K *et al.* (2016). Identification and correction of mechanisms underlying inherited blindness in human iPSC-derived optic cups. *Cell Stem Cell* **18**: 769–781.
49. Miller, TM, Pestronk, A, David, W, Rothstein, J, Simpson, E, Appel, SH *et al.* (2013). An antisense oligonucleotide against SOD1 delivered intrathecally for patients with SOD1 familial amyotrophic lateral sclerosis: a phase 1, randomised, first-in-man study. *Lancet Neurol* **12**: 435–442.
50. Koo, T and Wood, MJ (2013). Clinical trials using antisense oligonucleotides in duchenne muscular dystrophy. *Hum Gene Ther* **24**: 479–488.
51. Goemans, NM, Tulinius, M, van den Akker, JT, Burm, BE, Ekhart, PF, Heuvelmans, N *et al.* (2011). Systemic administration of PRO051 in Duchenne's muscular dystrophy. *N Engl J Med* **364**: 1513–1522.
52. Voit, T, Topaloglu, H, Straub, V, Muntoni, F, Deconinck, N, Campion, G *et al.* (2014). Safety and efficacy of drisapersen for the treatment of Duchenne muscular dystrophy (DEMAND II): an exploratory, randomised, placebo-controlled phase 2 study. *Lancet Neurol* **13**: 987–996.
53. Flanigan, KM, Voit, T, Rosales, XQ, Servais, L, Kraus, JE, Wardell, C *et al.* (2014). Pharmacokinetics and safety of single doses of drisapersen in non-ambulant subjects with Duchenne muscular dystrophy: results of a double-blind randomized clinical trial. *Neuromuscul Disord* **24**: 16–24.
54. Yu, FS and Hazlett, LD (2006). Toll-like receptors and the eye. *Invest Ophthalmol Vis Sci* **47**: 1255–1263.
55. Kumar, MV, Nagineni, CN, Chin, MS, Hooks, JJ and Detrick, B (2004). Innate immunity in the retina: Toll-like receptor (TLR) signaling in human retinal pigment epithelial cells. *J Neuroimmunol* **153**: 7–15.
56. Richardt-Pargmann, D and Vollmer, J (2009). Stimulation of the immune system by therapeutic antisense oligodeoxynucleotides and small interfering RNAs via nucleic acid receptors. *Ann N Y Acad Sci* **1175**: 40–54.
57. Kole, R and Krieg, AM (2015). Exon skipping therapy for Duchenne muscular dystrophy. *Adv Drug Deliv Rev* **87**: 104–107.
58. Aartsma-Rus, A, Kaman, WE, Weij, R, den Dunnen, JT, van Ommen, GJ and van Deutekom, JC (2006). Exploring the frontiers of therapeutic exon skipping for Duchenne muscular dystrophy by double targeting within one or multiple exons. *Mol Ther* **14**: 401–407.
59. Adams, AM, Harding, PL, Iversen, PL, Coleman, C, Fletcher, S and Wilton, SD (2007). Antisense oligonucleotide induced exon skipping and the dystrophin gene transcript: cocktails and chemistries. *BMC Mol Biol* **8**: 57.
60. Wilton, SD, Fall, AM, Harding, PL, McClorey, G, Coleman, C and Fletcher, S (2007). Antisense oligonucleotide-induced exon skipping across the human dystrophin gene transcript. *Mol Ther* **15**: 1288–1296.
61. Liu, X, Bulgakov, OV, Darrow, KN, Pawlyk, B, Adamian, M, Liberman, MC *et al.* (2007). Usherin is required for maintenance of retinal photoreceptors and normal development of cochlear hair cells. *Proceed Natl Acad Sci USA* **104**, 4413–4418.

62. Slijkerman, RW, Song, F, Astuti, GD, Huynen, MA, van Wijk, E, Stieger, K *et al.* (2015). The pros and cons of vertebrate animal models for functional and therapeutic research on inherited retinal dystrophies. *Prog Retin Eye Res* **48**: 137–159.
63. Wasfy, MM, Matsui, JI, Miller, J, Dowling, JE and Perkins, BD (2014). myosin 7aa(-/-) mutant zebrafish show mild photoreceptor degeneration and reduced electroretinographic responses. *Exp Eye Res* **122**: 65–76.
64. Phillips, JB, Blanco-Sanchez, B, Lentz, JJ, Tallafuss, A, Khanobdee, K, Sampath, S *et al.* (2011). Harmonin (Ush1c) is required in zebrafish Müller glial cells for photoreceptor synaptic development and function. *Dis Model Mech* **4**: 786–800.
65. Seiler, C, Finger-Baier, KC, Rinner, O, Makhankov, YV, Schwarz, H, Neuhauss, SC *et al.* (2005). Duplicated genes with split functions: independent roles of protocadherin15 orthologues in zebrafish hearing and vision. *Development* **132**: 615–623.
66. Ebermann, I, Phillips, JB, Liebau, MC, Koenekoop, RK, Schermer, B, Lopez, I *et al.* (2010). PDZD7 is a modifier of retinal disease and a contributor to digenic Usher syndrome. *J Clin Invest* **120**: 1812–1823.
67. Garanto, A, Duijkers, L and Collin, RW (2015). Species-dependent splice recognition of a cryptic exon resulting from a recurrent intronic CEP290 mutation that causes congenital blindness. *Int J Mol Sci* **16**: 5285–5298.
68. Raghava, S, Hammond, M and Kompella, UB (2004). Periocular routes for retinal drug delivery. *Expert Opin Drug Deliv* **1**: 99–114.
69. Janoria, KG, Gunda, S, Boddu, SH and Mitra, AK (2007). Novel approaches to retinal drug delivery. *Expert Opin Drug Deliv* **4**: 371–388.
70. Falzarano, MS, Passarelli, C and Ferlini, A (2014). Nanoparticle delivery of antisense oligonucleotides and their application in the exon skipping strategy for Duchenne muscular dystrophy. *Nucleic Acid Ther* **24**: 87–100.
71. Wada, S, Urase, T, Hasegawa, Y, Ban, K, Sudani, A, Kawai, Y *et al.* (2014). Aib-containing peptide analogs: cellular uptake and utilization in oligonucleotide delivery. *Bioorg Med Chem* **22**: 6776–6780.
72. Gedicke-Hornung, C, Behrens-Gawlik, V, Reischmann, S, Geertz, B, Stimpel, D, Weinberger, F *et al.* (2013). Rescue of cardiomyopathy through U7snRNA-mediated exon skipping in Mybpc3-targeted knock-in mice. *EMBO Mol Med* **5**: 1128–1145.
73. Geib, T and Hertel, KJ (2009). Restoration of full-length SMN promoted by adenoviral vectors expressing RNA antisense oligonucleotides embedded in U7 snRNAs. *PLoS One* **4**: e8204.
74. Goyenvalle, A, Vulin, A, Fougerousse, F, Leturcq, F, Kaplan, JC, Garcia, L *et al.* (2004). Rescue of dystrophic muscle through U7 snRNA-mediated exon skipping. *Science* **306**: 1796–1799.
75. Dalkara, D, Kolstad, KD, Caporale, N, Visel, M, Klimczak, RR, Schaffer, DV *et al.* (2009). Inner limiting membrane barriers to AAV-mediated retinal transduction from the vitreous. *Mol Ther* **17**: 2096–2102.
76. Kotterman, MA, Yin, L, Strazzeri, JM, Flannery, JG, Merigan, WH and Schaffer, DV (2015). Antibody neutralization poses a barrier to intravitreal adeno-associated viral vector gene delivery to non-human primates. *Gene Ther* **22**: 116–126.
77. Li, Q, Miller, R, Han, PY, Pang, J, Dinculescu, A, Chiodo, V *et al.* (2008). Intraocular route of AAV2 vector administration defines humoral immune response and therapeutic potential. *Mol Vis* **14**: 1760–1769.
78. Dalkara, D, Byrne, LC, Klimczak, RR, Visel, M, Yin, L, Merigan, WH *et al.* (2013). In vivo-directed evolution of a new adeno-associated virus for therapeutic outer retinal gene delivery from the vitreous. *Sci Transl Med* **5**: 189ra76.
79. Kremer, H, van Wijk, E, Märker, T, Wolfrum, U and Roepman, R (2006). Usher syndrome: molecular links of pathogenesis, proteins and pathways. *Hum Mol Genet* **15 Spec No 2**: R262–R270.
80. Reiners, J, van Wijk, E, Märker, T, Zimmermann, U, Jürgens, K, te Brinke, H *et al.* (2005). Scaffold protein harmonin (USH1C) provides molecular links between Usher syndrome type 1 and type 2. *Hum Mol Genet* **14**: 3933–3943.
81. Lentz, JJ, Jodelka, FM, Hinrich, AJ, McCaffrey, KE, Farris, HE, Spalitta, MJ *et al.* (2013). Rescue of hearing and vestibular function by antisense oligonucleotides in a mouse model of human deafness. *Nat Med* **19**: 345–350.
82. Reuter, JS and Mathews, DH (2010). RNAstructure: software for RNA secondary structure prediction and analysis. *BMC Bioinformatics* **11**: 129.
83. Yariz, KO, Duman, D, Seco, CZ, Dallman, J, Huang, M, Peters, TA *et al.* (2012). Mutations in OTOGL, encoding the inner ear protein otogelin-like, cause moderate sensorineural hearing loss. *Am J Hum Genet* **91**: 872–882.

Supplementary Information accompanies this paper on the Molecular Therapy–Nucleic Acids website (http://www.nature.com/mtna)